

ScienceDirect



IFAC PapersOnLine 58-28 (2024) 1097-1102

Nullspace Adaptive Identification of Plant and Actuator Model Parameters for Underactuated Ground Vehicles: Theory and Experimental Evaluation*

Allan H. Elsberry *,** Jeremy J. Dawkins * Annie M. Mao ** Louis L. Whitcomb **

* Department of Weapons, Robotics, and Control Engineering United, States Naval Academy, Annapolis, MD 21401, USA, (e-mail: elsberry@usna.edu, dawkins@usna.edu). ** Department of Mechanical Engineering, Johns Hopkins University Baltimore, MD 21218, USA,(e-mail: amao1@jhu.edu, llw@jhu.edu)

Abstract: This paper reports a novel Nullspace Adaptive Identification (NSAID) algorithm to estimate plant and actuator model parameters for an underactuated ground vehicle with dynamics represented by a 3 degree-of-freedom second-order dynamic model, and reports an evaluation of its performance in simulation and experiments. Precise identification of ground vehicle plant and actuator model parameters is critical for physically realistic model-based simulation, control, navigation, and fault detection. However, ground vehicle plant model parameters, such as vehicle mass, moments of inertia, tire cornering stiffness and actuator model parameters such as motor torque constants are generally not possible to estimate a priori from first principles, and can change with varying payloads, configurations, and driving environments, and thus must be determined experimentally. Some parameter identification methods such as least squares regression depend on acceleration measurements, and most identification methods assume a priori knowledge of actuator parameters. In contrast, NSAID estimates plant and actuator parameters simultaneously, does not require acceleration measurements, can be utilized offline or online during vehicle operation, and can be applied with open or closed-loop control.

Copyright © 2024 The Authors. This is an open access article under the CC BY-NC-ND license (https://creativecommons.org/licenses/by-nc-nd/4.0/)

Keywords: Nonlinear Adaptive Control, Vehicle Dynamics, Model Parameter Identification

1. INTRODUCTION

Accurate dynamical models for ground vehicles are useful for a variety of applications including the following: (1) Forward Simulation and Testing: New control systems can be refined within a simulated environment that utilizes a vehicle's dynamical model prior to being deployed to resource-intensive hardware trials. (2) Model-Based Control and Navigation Systems: Dynamical plant and actuator models can be incorporated into model-based control and navigation systems to provide improved performance in comparison to conventional non-model-based approaches (Kiencke and Nielsen, 2005). (3) Safer Driver Assistance Systems: Instead of using sensors alone to warn or react to an operator's input, dynamical models can be used to adjust operator commands such that the vehicle always remains in a safe operational envelope (Holzmann et al., 2006). (4) Fault Detection: Model-based fault detection and isolation techniques can use knowledge of a system's dynamics to localize faults (Mao and Whitcomb, 2021). (5) Robust State Estimation: Dynamical Models are useful for estimating vehicle states that can not be exactly measured due to sensor limitations (Sen et al., 2015).

Experimentally determining precise model parameter values for a vehicle can be a formidable challenge. Plant parameters such as mass and moments of inertia are subject to change based on the vehicle's physical configuration and payload requirements. Actuator parameters such as electric motor torque constants are susceptible to variations based on the operating environment (Ali et al., 2016). Tire friction data is seldom provided by manufacturers, and tire performance can vary due to factors including tire wear and driving surface conditions (Rajamani, 2012).

This paper addresses the estimation of plant and actuator parameter values for a commonly accepted second-order, nonlinear, three Degree-of-Freedom (3-DOF), linear-in-the-parameters ground vehicle dynamical model. As is the case with many vehicles, most of the plant and actuator model parameters are not known a priori. The value of many of these parameters are generally not possible to estimate analytically from first principles and, as a result, these model parameters must be determined experimentally.

This study reports a novel Nullspace Adaptive Identification (NSAID) algorithm to estimate both plant and actuator parameter values for a widely accepted ground vehicle dynamical model. We report the first simulation and experimental evaluation of the performance of the NSAID algorithm in achieving parameter identification for a ground vehicle model. This approach relies solely upon knowledge of the control input signals and vehicle body-velocity measurement signals, without requiring acceleration signals or sensing.

The remainder of this paper is organized as follows: Section 2 reviews previous literature. Section 3 reviews the ground vehicle plant and actuator model and presents a

^{*} We gratefully acknowledge the support of the U.S. Navy (Elsberry, Dawkins), the JHU William F. Ward, Jr. Fellowship (Elsberry), the National Science Foundation under Award 1909182 (Whitcomb), and a Johns Hopkins University Applied Physics Laboratory (JHU APL) Graduate Fellowship (Mao).

new adaptive NSAID identifier for this model, an extension of the approach reported in (Harris et al., 2023). Section 4 reports the results of a numerical simulation study employing the NSAID algorithm and compares the estimated parameter values to their true values. Section 5 reports the results of an experimental evaluation which uses data from a 1/10th scale ground vehicle and NSAID to estimate model parameter values. Section 6 summarizes and concludes.

2. LITERATURE REVIEW

Vehicle parameter estimation consists broadly of two approaches: sensor-based and model-based methods. Sensorbased methods involve the incorporation of additional sensors into a vehicle design to monitor the value of specific parameter(s) of interest, (Reina et al., 2017). In (Erdogan et al., 2011) the authors report a method of determining the tire-road friction coefficient by using a specialized piezoelectric sensor embedded in a tire. Since most vehicles and components do not come equipped with additional specialized sensors, implementing sensor-based methods can be challenging and costly.

Model-based methods use the signals from existing vehicle sensor data in conjunction with vehicle control input signals to estimate parameters. Least Squares (LS) is one method that can be used to estimate model parameters from experimental data. Recursive Least Squares (RLS) identification has also been used for vehicle parameter estimation and can be used for iterative, online updates while the vehicle is operating (Rajamani, 2012). However, both LS and RLS methods require linear and rotational acceleration measurements to determine parameters in second order dynamic models. The disadvantage is that linear acceleration signals, commonly acquired by differentiating velocity measurements or using acceleration sensors, are prone to noise. Even with dedicated acceleration sensors, the true body-acceleration signal is obscured by the gravitational acceleration acting on a vehicle body frame with dynamic attitude. In (Vahidi et al., 2005), the authors report a model-based method for measuring vehicle mass and road grade and note that "the signals recorded from the accelerometers were noisy and therefore we decided not to use these signals for obtaining accelerations.

Kalman Filters (KF) have also been used to estimate ground vehicle model parameters. In (Bevly et al., 2006) the authors report on a Kalman Filter approach used to estimate tire slip angles. The authors also note issues with linear acceleration measurement error and report a kinematic Kalman Filter method to improve the acceleration measurements that were ultimately used to estimate the tire cornering stiffness model parameters.

The NSAID approach differs from model-based parameter estimation methods such as LS and KF methods in that it does not require acceleration measurements and has been analytically proven to guarantee parameter convergence to the set of true parameters (Harris et al., 2023).

3. BICYCLE MODEL AND NSAID ALGORITHM

Section 3.1 reviews a commonly accepted vehicle dynamics model. Section 3.2 reports an NSAID algorithm for this plant model. Section 3.3 outlines the Lyapunov stability proof of the NSAID algorithm.

3.1 Ground Vehicle Bicycle Dynamics Model

A 3-DOF ground vehicle dynamical model where the lateral and heading (i.e. steering) dynamics use the commonly accepted "Bicycle Model" takes the form

Table 1. Variable Definitions and units

<u></u>	Longitudinal velocity (Body-frame)	m/s
$\dot{\dot{y}}$	Lateral velocity (Body-frame)	m/s
$\dot{\psi}$	Yaw rate (Body-frame)	rad/s
$I_m^{^{ au}}$	Motor Current	A
δ	Front tire steering angle	rad

Table 2. Parameter Definitions, Units, and (A)ctuator / (P)lant Designation

l_f	Distance, center of mass to front wheel	m	Р
l_r	Distance, center of mass to rear wheel	m	Ρ
m	Vehicle mass	kg	Ρ
J_z	z-axis moment of inertia	$kg \cdot m^2$	Ρ
K_t	Motor drive-train torque constant	N/A	A
C_{rr}	Rolling resistance coefficient	$N \cdot s/m$	Ρ
$C_{\alpha f}$	Front tire cornering stiffness	N/rad	Α
$C_{\alpha r}$	Rear tire cornering stiffness	N/rad	Ρ
C_{Δ}	$C_{\alpha f} + C_{\alpha r}$	N/rad	Ρ
C_{Σ}	$C_{\alpha f} - C_{\alpha r}$	N/rad	Р

$$\ddot{x} = K_t \frac{I_m}{m} - \frac{C_{rr}\dot{x}}{m} + \dot{y}\dot{\psi} \tag{1}$$

$$\ddot{y} = -\frac{C_{\alpha f} + C_{\alpha r}}{m\dot{x}}\dot{y} - \frac{C_{\alpha f}l_f - C_{\alpha r}l_r}{m\dot{x}}\dot{\psi} + \frac{C_{\alpha f}}{m}\delta - \dot{x}\dot{\psi} \quad (2)$$

$$\ddot{y} = -\frac{C_{\alpha f} + C_{\alpha r}}{m\dot{x}}\dot{y} - \frac{C_{\alpha f}l_f - C_{\alpha r}l_r}{m\dot{x}}\dot{\psi} + \frac{C_{\alpha f}}{m}\delta - \dot{x}\dot{\psi}$$
(2)
$$\ddot{\psi} = -\frac{C_{\alpha f}l_f - C_{\alpha r}l_r}{J_z\dot{x}}\dot{y} - \frac{C_{\alpha f}l_f^2 + C_{\alpha r}l_r^2}{J_z\dot{x}}\dot{\psi} + \frac{C_{\alpha f}l_f}{J_z}\delta$$
(3)

where the longitudinal dynamics of the body (1) has the control input of motor current in Amperes, $I_m(t)$, and the lateral dynamics (2) and heading dynamics (3) have the control input of front tire steering angle $\delta(t)$. The remaining variables and plant and actuator parameters in (1)-(3) are defined in, respectively, Tables 1 and 2. We note that (2) and (3) represent the commonly accepted bicycle vehicle dynamics model as reported in (Rajamani, 2012).

 C_{Σ} and C_{Δ} can be defined as follows

$$C_{\Sigma} \triangleq C_{\alpha f} + C_{\alpha r} \tag{4}$$

$$C_{\Delta} \triangleq C_{\alpha f} - C_{\alpha r}.\tag{5}$$

and substituted into (2) and (3) for brevity. We note that $C_{\alpha f}$ remains in our modified model as it acts as an actuator parameter while C_{Σ} and C_{Δ} represent plant parameters

The center of mass for our vehicle is located in center of the longitudinal axis of the vehicle frame such that

$$l_f = l_r = l. (6)$$

Our simplified vehicle equations of motion take the form

$$\ddot{x} = K_t \frac{I_m}{m} - \frac{C_{rr}\dot{x}}{m} + \dot{y}\dot{\psi} \tag{7}$$

$$\ddot{y} = -\frac{C_{\Sigma}}{m\dot{x}}\dot{y} - \frac{C_{\Delta}l}{m\dot{x}}\dot{\psi} + \frac{C_{\alpha f}}{m}\delta - \dot{x}\dot{\psi}$$
 (8)

$$\ddot{\psi} = -\frac{C_{\Delta}l}{J_z \dot{x}} \dot{y} - \frac{C_{\Sigma}l^2}{J_z \dot{x}} \dot{\psi} + \frac{C_{\alpha f}l}{J_z} \delta. \tag{9}$$

Defining v as the velocity state vector as

$$v \triangleq \begin{bmatrix} \dot{x} \ \dot{y} \ \dot{\psi} \end{bmatrix}^T \tag{10}$$

results in the final body-frame velocity dynamics

$$\dot{v} = \begin{bmatrix} \ddot{x} \\ \ddot{y} \\ \ddot{y} \end{bmatrix} = \begin{bmatrix} K_t \frac{I_m}{m} - \frac{C_{rr}\dot{x}}{m} + \dot{y}\dot{\psi} \\ -\frac{C_{\Sigma}}{m\dot{x}}\dot{y} - \frac{C_{\Delta}l}{m\dot{x}}\dot{\psi} + \frac{C_{\alpha f}}{m}\delta - \dot{x}\dot{\psi} \\ -\frac{C_{\Delta}l}{J_z\dot{x}}\dot{y} - \frac{C_{\Sigma}l^2}{J_z\dot{x}}\dot{\psi} + \frac{C_{\alpha f}l}{J_z}\delta \end{bmatrix}.$$
(11)

3.2 NSAID Algorithm

We define the parameter vector, $\theta \in \mathbb{R}^{7 \times 1}$, as

$$\theta \triangleq \left[m \ J_z \ K_t \ C_{rr} \ C_{\alpha f} \ C_{\Sigma} \ C_{\Delta} \right]^T, \tag{12}$$

composed of the model's plant and actuator parameters. We define the positive definite inertia matrix, M, as

$$M(\theta) = \begin{bmatrix} m & 0 & 0 \\ 0 & m & 0 \\ 0 & 0 & J_z \end{bmatrix}. \tag{13}$$

Factoring out $M^{-1}(\theta)$ from (11) and taking the Jacobian with respect to θ , results in an expression of the form

$$\dot{v}(\theta) = M^{-1}(\theta)W_{\dot{v}}(v,\xi)\theta\tag{14}$$

where \dot{v} is a function $W_{\dot{v}}(v,\xi)$ collects the nonlinear terms due to v and $\xi \triangleq [I_m \ \delta]^T$, the vector of control inputs.

Rearranging all terms to the right hand side and using the using Jacobian operator, D_{θ} , which is defined such that $p(\theta) = D_{\theta}[p(\theta)]\theta$, we can factor out the regressor matrix-valued function $\mathbb{W}(\dot{v}, v, \xi) \in \mathbb{R}^{3 \times 7}$

$$0 = D_{\theta}[M(\theta)\dot{v}(\theta) - W_{\dot{v}}(v,\xi)\theta]\theta \tag{15}$$

$$0 = \mathbb{W}(\dot{v}, v, \xi)\theta \tag{16}$$

where $\mathbb{W}(\dot{v}, v, \xi)$ takes the following form

$$\mathbb{W}(\dot{v}, v, \xi) = \begin{bmatrix} \ddot{x} - \dot{\psi}\dot{y} & 0 & -I_m \ \dot{x} & 0 & 0 & 0 \\ \ddot{y} + \dot{\psi}\dot{x} & 0 & 0 & 0 -\delta \ \dot{y}/\dot{x} & l\dot{\psi}/\dot{x} \\ 0 & \ddot{\psi} & 0 & 0 -l\delta \ l^2\dot{\psi}/\dot{x} \ l\dot{y}/\dot{x} \end{bmatrix} . (17)$$

Note that (16) shows that $\theta \in null(\mathbb{W}(\dot{v}, v, \xi))$ and that the 'true' θ that persistently satisfies (16) is not only one single point in parameter space, but rather any element θ^* of the set $P(\theta)$, where

$$P(\theta) \triangleq \{\theta^* \in \mathbb{R}^7 : \theta^* \neq 0 \text{ and }$$

$$W(\dot{v}, v, \xi)\theta = 0 \iff W(\dot{v}, v, \xi)\theta^* = 0\}.$$
 (18)

As an example, it is easy to see that any scalar multiple of θ equivalently satisfies the nullspace relationship (16). We define the parameter estimate $\hat{\theta}$, the identification plant \hat{v} , and the following error coordinates

$$\Delta\theta \triangleq \hat{\theta} - \theta \tag{19}$$

$$\Delta v \triangleq \hat{v} - v. \tag{20}$$

We choose an adaptive identification plant of the form

$$\dot{\hat{v}} \triangleq \dot{v}(\hat{\theta}) - \mathcal{A}\Delta v \tag{21}$$

where $\mathcal{A} \in \mathbb{R}^{3\times3}$ is a positive definite symmetric gain matrix and $\dot{v}(\hat{\theta})$ is the resulting time-derivative of the body velocity as a function of the estimated parameters $\hat{\theta}$ instead of the true parameters θ (14), defined as

$$\dot{v}(\hat{\theta}) \triangleq M^{-1}(\hat{\theta})W_{\dot{v}}(v,\xi)\hat{\theta}. \tag{22}$$

The NSAID parameter update law is

$$\dot{\hat{\theta}} \triangleq \Gamma \mathbb{W}(\dot{v}(\hat{\theta}), v, \xi)^T \Delta v. \tag{23}$$

where $\Gamma \in \mathbb{R}^{7 \times 7}$ is a positive definite symmetric parameter adaptation gain matrix and $\mathbb{W}(\dot{v}(\hat{\theta}), v, \xi)$ is the regressor matrix-valued function (17) with $\dot{v}(\hat{\theta})$ (22) as its argument instead of the true time-derivative of body velocity $\dot{v}(\theta)$ (14).

3.3 NSAID Lyapunov Stability Analysis

This Section presents an outline of the Lyapunov stability proof for the NSAID algorithm.

After evaluation of our error systems, $\Delta \dot{v}$ and $\Delta \dot{\theta}$, we define a new error state vector for Lyapunov analysis, $z \triangleq [\Delta v \Delta \theta]^T$, whose dynamics are computed from (14,21,23),

define a few error state vector for Lyapunov analysis,
$$z = [\Delta v \ \Delta \theta]^T$$
, whose dynamics are computed from $(14,21,23)$,
$$\dot{z} = \begin{bmatrix} \Delta \dot{v} \\ \Delta \dot{\theta} \end{bmatrix} = \begin{bmatrix} -\mathcal{A}_{3\times3} & -M(\theta)^{-1} \mathbb{W}(\dot{v}(\hat{\theta}, v, \xi)_{3\times7}] \\ \Gamma \mathbb{W}(\dot{v}(\hat{\theta}))_{7\times3}^T & 0_{7\times7} \end{bmatrix} z$$
(24)

We separate (24) into block matrices

$$E = E^{T} = \begin{bmatrix} M_{3\times3}^{-1}(\theta) & 0_{3\times7} \\ 0_{7\times3} & \Gamma_{7\times7} \end{bmatrix},$$
 (25)

$$F = -F^{T} = \begin{bmatrix} 0_{3\times3} & -\mathbb{W}(\dot{v}(\hat{\theta}, v, \xi))_{3\times7} \\ \mathbb{W}(\dot{v}(\hat{\theta}, v, \xi)_{7\times3}^{T} & 0_{7\times7} \end{bmatrix}, (26)$$

and

$$G = G^{T} = \begin{bmatrix} -\mathcal{A}_{3\times3} & 0_{3\times7} \\ 0_{7\times3} & 0_{7\times7} \end{bmatrix}, \tag{27}$$

where E is positive definite symmetric, F is skew-symmetric, and G is negative semi-definite symmetric, such that $\dot{z} = (EF + G)z$. Evaluating the following candidate Lyapunov function

$$V(z) = \frac{1}{2}z^T E^{-1}z > 0 (28)$$

which satisfies V(0)=0 and $V(z)>0 \ \forall z\neq 0$, and taking the derivative using properties of $E,\,F,$ and G yields

$$\dot{V}(z) = z^T (GE^{-1})z \le 0 (29)$$

where $\dot{V}(0) = 0$ and \dot{V} is negative definite in Δv and negative semi-definite overall in z. From this it can be shown that all signals are bounded, that the system (24) is locally uniformly stable about the origin, and that $\lim_{t\to\infty} \Delta v(t) = 0$. An additional persistence of excitation (PE) condition reported in (Harris et al., 2023) further guarantees asymptotic convergence of the parameter estimate $\hat{\theta}$ to the true parameter set $P(\theta)$ (18).

4. NSAID SIMULATION EVALUATION

This Section reports an evaluation of the NSAID algorithm (21,23) applied to a simulated model of a ground vehicle with dynamics given by (11). The true parameter vector employed in the simulation was $\theta = [3.15, 0.02, 0.1, 0.2, 15, 60, -45]^T$. We selected and simulated open loop throttle and steering inputs such that

- (1) the resulting state velocities have similar magnitudes to the ground vehicle used in the experimental evaluation, and
- (2) the PE requirement is satisfied (Harris et al., 2023).

Table 3 lists the simulation open-loop control input signals. The seven plant model parameter estimates were initial-

Table 3. Simulation Control Inputs

$$I_m(t) = 2 + 4sin(0.91t)$$

$$\delta(t) = 0.25sin(0.73t) + 0.05sin(0.11t)$$

ized to within $\pm 10\%$ of their true values. The gain values used in (21) and (23) were

$$\Gamma = \text{diag}(0.3 \ 0.002 \ 0.003 \ 0.003 \ 0.3 \ 21 \ 21)$$
 (30)

$$A = diag(0.21 \ 0.3 \ 0.9). \tag{31}$$

Figure 1 shows that the normalized estimated parameter vector converges to the true parameter vector, confirming that $\lim_{t\to\infty} \hat{\theta}(t) \in P(\theta)$.

Figure 2 shows that the identification plant velocity converges to the plant velocity, i.e. $\lim_{t\to\infty} \Delta v(t) = 0$.

Adjusting the Γ gains to higher values allows for faster parameter convergence in simulation. However, large parameter gain values can lead to undesirable parameter estimate oscillations. The gain values in this simulation are comparable to those used in the experimental trials and produce minimal oscillation as shown in Figure 1.

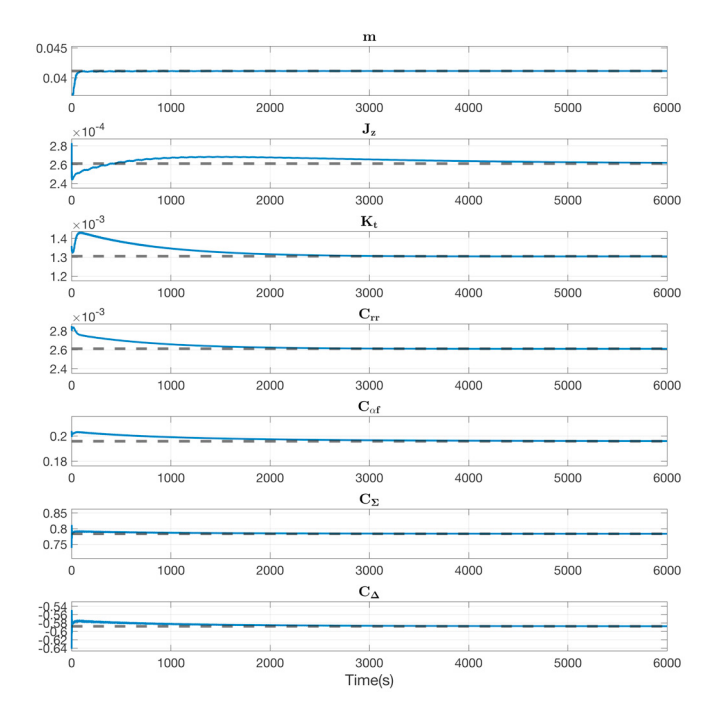


Fig. 1. Parameter Convergence, Simulated Ground Vehicle: Plot of normalized parameter estimates compared to the normalized actual model parameters. Each parameter estimate was initialized with an offset between -10% to +10% of its 'true' value. During the simulation, the normalized value of each parameter converges to the normalized true parameter value.

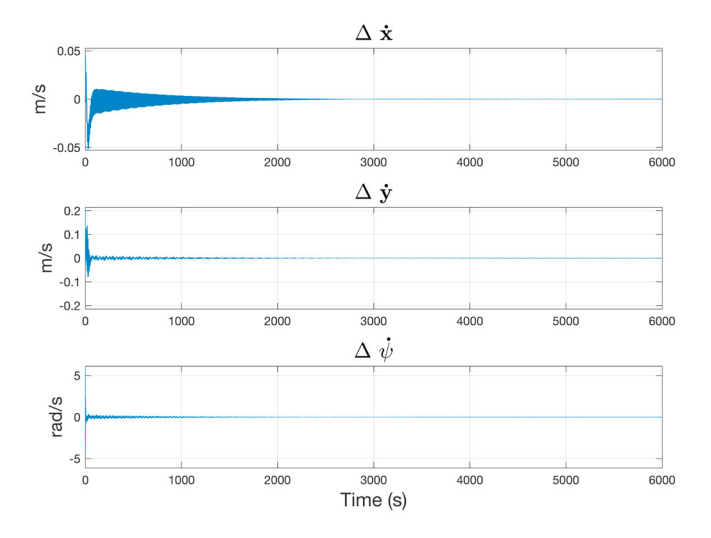


Fig. 2. Velocity Convergence, Simulated Ground Vehicle: Each component of Δv during the simulation, showing that the identification plant error converges to 0.

5. NSAID EXPERIMENTAL EVALUATION

This Section reports the equipment and processes used to experimentally evaluate the NSAID algorithm performance. Section 5.1 describes the experiment setup and data collection methods, Section 5.2 reports of the experimental evaluation of the NSAID algorithm. Section 5.3 reports the LS methodology performance comparison.

5.1 Ground Vehicle Experimental Setup

We used a brushless radio-controlled 1/10th scale model car, pictured in Figure 3, for the experiments. The vehicle

mass was 3.15 kg and the length from the front to rear axles was 0.28m. The center of gravity was measured to be at the longitudinal center of the front and rear axles.

A Vedder's Electronic Speed Controller (VESC Project, Benjamin Vedder) received velocity commands from the hand-controller and logged the current delivered to the motor at 50 Hz, which was used as the $I_m(t)$ input. A servo connected to the front wheels provided steering, and the steering servo command was logged at 100 Hz and mapped to a steering angle as the input $\delta(t)$.

A BNO055 (Bosch Sensortec, Reutlingen, Germany) absolute orientation sensor was utilized to record the yaw rate, $\dot{\psi}(t)$. The experiment took place inside of a laboratory outfitted with a Qualisys 7+ Series Motion Capture System (Qualisys, Göteborg, Sweden) capable of recording 3D position and orientation at up to 300 frames-per-second. For these experiments, the 3D position and orientation values were captured, differentiated, and converted to body-frame velocities at 33Hz to produce estimates for $\dot{x}(t)$ and $\dot{y}(t)$. The car was manually driven with a hand controller for



Fig. 3. 1/10 Scale model ground vehicle

a 15-minute training drive (Training Drive Dataset) and for a 5-minute validation drive (Validation Drive Dataset). During these operations, the following priorities were considered:

- (1) Staying within the confines of the room where motion capture logging is available,
- (2) Ensuring that the longitudinal velocity \dot{x} always remained positive to avoid division-by-zero issues in the bicycle model, (2) and (3).
- (3) Providing frequent turns in both directions to create a PE steering input, and
- (4) Providing speed changes to create a PE current input.

While issuing frequently changing steering commands was straightforward, the limited $9.7~\mathrm{m} \times 6.7~\mathrm{m}$ operational area constrained the feasible magnitudes of vehicle velocity, and limited velocity changes. After the experimental drives were completed, the velocity and control signals were resampled by linear interpolation to $200\mathrm{Hz}$.

5.2 NSAID Experimental Performance Evaluation

Unlike in the simulation vehicle reported in Section 4, the true parameters of our experimental vehicle are mostly unknown. The vehicle and additional sensors have been custom-assembled, and tire friction parameters are unknown. The only model parameter that we could directly measure was the mass of the vehicle. In order to evaluate the performance of the NSAID algorithm, we performed the following steps using the Training Drive Dataset:

(1) We ran the NSAID algorithm through the training data until the normalized NSAID estimated parameter vector converged to constant values.

- (2) We performed LS regression to generate a LS estimated parameter vector as a comparison. Section 5.3 presents the LS parameter estimation methods.
- (3) We used the resulting converged parameter estimates to compute forward simulations of the model.
- (4) We compared the NSAID and LS simulation velocities to the experimentally collected velocity data.

Euler integration was used to apply the NSAID algorithm at each 0.005 second time step of the training drive data. Each parameter was initialized to the final estimate of the previous iteration, and the algorithm was executed for 20 iterations over the full 15-minute training dataset.

The final parameter estimate values are shown in Table 4. Due to the non-uniqueness of true parameter values in $P(\theta)$ as discussed in Section 3.2, a direct comparison to the LS estimate is not meaningful without normalization. Instead, we evaluate the performance of the two parameter sets in predicting vehicle velocities during forward simulation.

Table 4. Comparison of Estimated Parameters

Parameter	NSAID	NSAID	LS Estimate	Units
	Initial	Converged		
	Estimate	Estimate		
\overline{m}	3.15	3.09	3.15	kg
J_z	0.1	0.0481	0.0335	$kg \cdot m^2$
K_t	0.1	0.200	0.197	N/A
C_{rr}	0.1	0.502	0.629	$N \cdot s/m$
$C_{af} \ C_{\Sigma}$	10	8.01	7.11	N/rad
$C_{\Sigma}^{\ ec{\imath}}$	10	25.0	120.1	N/rad
C_{Δ}	-10	-41.6	-127.7	N/rad

To evaluate the NSAID identified parameter values, we used ODE45 to run a forward simulation of the vehicle model using the parameter values shown in Table 4 and the control inputs recorded during the experiment. Figure 4 shows a comparison of the simulated bicycle model velocities with both NSAID and LS estimated parameters and the experimentally recorded velocities during a 50 second segment of the Training Drive Dataset. The forward simulated lateral velocity, \dot{x} , performance is fair, but we conjecture simulated \dot{x} tracking performance might be improved with more accurate motor-current sensing and a more dynamic variation in the motor control signal. However, the forward simulation of \dot{y} , and $\dot{\psi}$ using NSAID adaptively estimated parameters closely matches the experimentally measured vehicle velocities.

For cross-validation, we performed a forward simulation on the Validation Drive Dataset using parameters identified with the Training Drive Dataset. Figure 5 compares the velocities resulting from both the NSAID and LS estimated model parameters to the experimentally-recorded velocities from the Validation Drive Dataset. The NSAID parameters in Table 4 provide a similar performance in modeling both the training and validation driving data.

The NSAID parameter estimate's rate of convergence improves when the estimated parameters are initialized closer to their 'true' values. Figure 6 shows the convergence of all parameter values to their previous adaptively identified values within 4000 seconds after J_z , $C_{\alpha f}$, and C_{Σ} were initialized to 90%, 110% and 90% of their previously identified values, respectively.

5.3 LS Methods and Experimental Performance Evaluation

We used Least Squares (LS) to estimate both plant and actuator parameters for our experimental ground vehicle with signals collected during the 15-minute training drive.

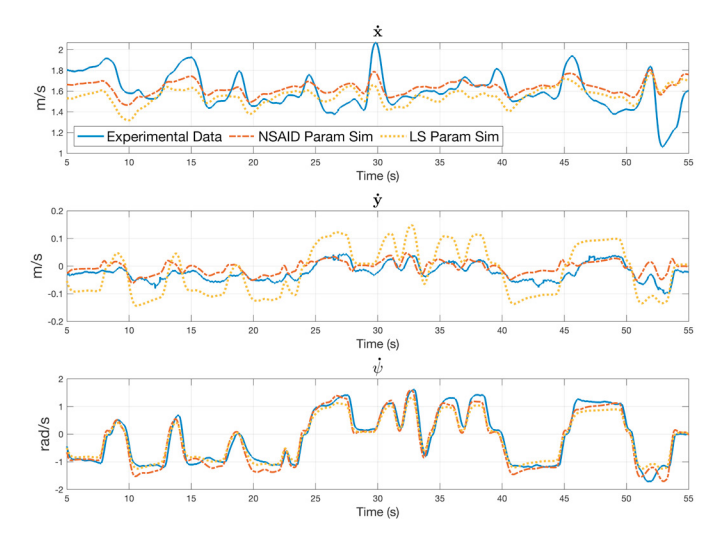


Fig. 4. Ground Vehicle Velocity, Training Dataset: Forward simulation model velocities with NSAID and LS estimated parameters compared to experimentally-measured training dataset velocities

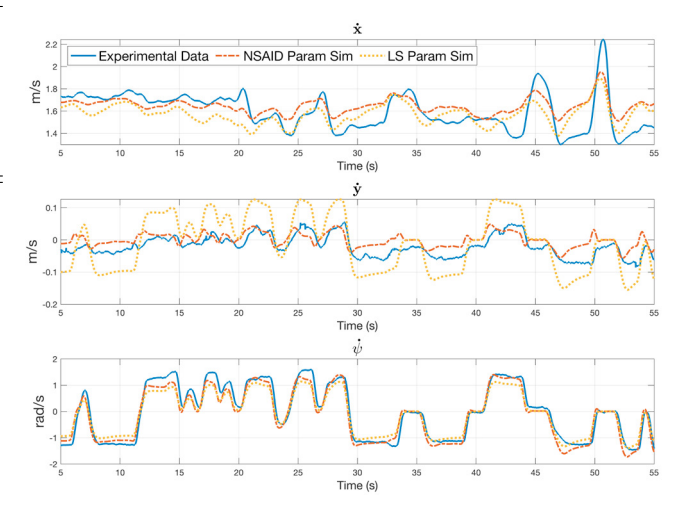


Fig. 5. Ground Vehicle Velocity, Validation Dataset: Forward simulation model velocities with NSAID and LS estimated parameters compared to experimentally-measured validation dataset velocities

For the LS parameter estimation we used the same input signals, $\xi \triangleq [I_m(t) \ \delta(t)]^T$, and velocity signals $v(t) \triangleq [\dot{x}(t) \ \dot{y}(t) \ \dot{\psi}(t)]^T$ described in Section 5.1. Additionally, we used the acceleration signals $\dot{v}(t) = [\ddot{x}(t) \ \ddot{y}(t) \ \ddot{\psi}(t)]$, where $\ddot{x}(t)$ and $\ddot{y}(t)$, were collected directly from the Bosch BNO055 and $\ddot{\psi}(t)$, was generated by differentiating the yaw rate signal from the BNO055. All signals were resampled with interpolation at 200Hz and accelerometer bias was removed from $\ddot{x}(t)$ and $\ddot{y}(t)$ by subtracting the mean of 300 samples of $\ddot{x}(t)$ and $\ddot{y}(t)$ while the vehicle was motionless.

Following the approach of (Harris et al., 2018) we used the regressor, $\mathbb{W}(\dot{v}, v, \xi)$ from (17) to determine the LS solution for θ by solving the following minimization

$$\min_{\theta} \left\{ ||\overline{\mathbb{W}}\theta||_2 : ||\theta||_2 = 1 \right\}. \tag{32}$$

This solution to the minimization problem was then scaled using the known value of mass (3.15 kg) and is shown in Table 4. As the true values of most of our model param-

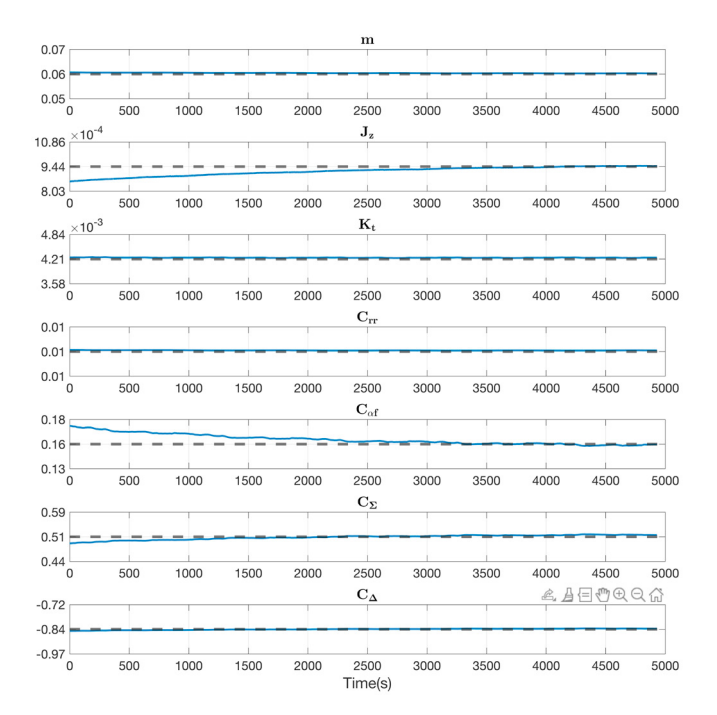


Fig. 6. Ground Vehicle Experimental NSAID Parameter Convergence: Plot of normalized estimate parameter values vs time showing parameters converging to their previously adaptively identified values.

eters are unknown, we compare the LS and NSAID estimated parameter performance with forward simulations of the training data and validation data in Figures 4 and 5. The Mean Squared Error (MSE), of actual experimental velocity data and forward simulation velocity using LS and NSAID estimated parameters for the training drive experiment is shown in Table 5.

5.4 Comparison of NSAID and LS Parameter Identification

While the longitudinal velocity, \dot{x} , performances are similar, the NSAID estimated model parameters produce a more accurate simulation of the ground vehicle's experimental \dot{y} and $\dot{\psi}$ velocities. The larger MSE seen in the LS estimated parameter forward simulation, particularly in the lateral velocity state, \dot{y} , likely highlights one of the methods' main disadvantages: LS parameter estimation requires linear acceleration data. With dynamic operation in a 3D environment or even a vehicle operating on a flat surface with sensitive shocks on each wheel, linear acceleration signals may be distorted by gravity.

Table 5. Comparison of Forward Simulation Mean Squared Error (MSE)

Dataset	State	NSAID MSE	LS MSE	Units
Training	\dot{x}	1.98×10^{-2}	3.45×10^{-2}	$(m/s)^2$
Training	\dot{y}	$6.96 imes10^{-4}$	39.7×10^{-4}	$(m/s)^2$
Training	$\dot{\psi}$	$4.76 imes 10^{-2}$	5.21×10^{-2}	$(rad/s)^2$
Validation	\dot{x}	3.40×10^{-2}	$2.83 imes 10^{-2}$	$(m/s)^2$
Validation	\dot{y}	$1.13 imes10^{-3}$	2.71×10^{-3}	$(m/s)^2$
Validation	$\dot{\psi}$	$6.97 imes10^{-2}$	7.18×10^{-2}	$(rad/s)^2$

6. CONCLUSIONS

This paper reports a novel Nullspace Adaptive Identification (NSAID) algorithm to perform simultaneous plant

and actuator parameter estimation on an underactuated 3-DOF ground vehicle dynamics model with both simulation and experimental evaluation. This NSAID approach can be extended to full 6-DOF dynamical ground vehicle models and, in contrast to well-known existing parameter identification methods, NSAID can be utilized without the need for acceleration measurements and without exact prior knowledge of actuator parameters. NSAID can be used with open-loop or closed-loop control and provides analytical guarantees of asymptotic parameter convergence if a persistence of excitation (PE) condition is satisfied.

We reported simulation studies showing asymptotic convergence of the parameter estimate to the true parameter set $P(\theta)$, and an experimental evaluation of the performance of NSAID of a ground vehicle, showing that a model using adaptively estimated parameters can accurately predict experimentally observed vehicle velocities.

REFERENCES

Ali, S., Hanif, A., and Ahmed, Q. (2016). Review in thermal effects on the performance of electric motors. In 2016 International Conference on Intelligent Systems Engineering (ICISE), 83–88. DOI:10.1109/INTELSE.2016.7475166.

Bevly, D.M., Ryu, J., and Gerdes, J.C. (2006). Integrating INS sensors with GPS measurements for continuous estimation of vehicle sideslip, roll, and tire cornering stiffness. *IEEE Transactions on Intelligent Transportation Systems*, 7(4), 483–493. DOI:10.1109/TITS.2006.883110.

Erdogan, G., Alexander, L., and Rajamani, R. (2011). Estimation of tire-road friction coefficient using a novel wireless piezo-electric tire sensor. *IEEE Sensors Journal*, 11(2), 267–279. DOI:10.1109/JSEN.2010.2053198.

Harris, Z.J., Mao, A.M., Paine, T.M., and Whitcomb, L.L. (2023). Stable nullspace adaptive parameter identification of 6 degree-of-freedom plant and actuator models for underactuated vehicles: Theory and experimental evaluation. The International Journal of Robotics Research, 42(12), 1070–1093. DOI:10.1177/02783649231191184.

Harris, Z.J., Paine, T.M., and Whitcomb, L.L. (2018). Preliminary evaluation of null-space dynamic process model identification with application to cooperative navigation of underwater vehicles. In 2018 IEEE/RSJ International Conference on Intelligent Robots and Systems (IROS), 3453–3459. DOI:10.1109/IROS.2018.8594257.

Holzmann, F., Bellino, M., Spiegelberg, G., and Sulzmann, A. (2006). Improvement of the driving safety using a predictive vehicle dynamical model. In 2006 IEEE International Conference on Vehicular Electronics and Safety, 289–294. DOI:10.1109/ICVES.2006.371601.

Kiencke, U. and Nielsen, L. (2005). Automotive Control Systems: For Engine, Driveline, and Vehicle. Springer Berlin, Heidelberg. DOI:10.1007/b137654.

Mao, A.M. and Whitcomb, L.L. (2021). A novel quotient space approach to model-based fault detection and isolation: Theory and preliminary simulation evaluation. In 2021 IEEE/RSJ International Conference on Intelligent Robots and Systems (IROS), 7119–7126. DOI:10.1109/IROS51168.2021.9636026.

Rajamani, R. (2012). Vehicle Dynamics and Control. Springer US. DOI:10.1007/978-1-4614-1433-9.

Reina, G., Paiano, M., and Blanco-Claraco, J.L. (2017). Vehicle parameter estimation using a model-based estimator. Mechanical Systems and Signal Processing, 87, 227–241. DOI:10.1016/j.ymssp.2016.06.038.

Sen, S., Chakraborty, S., and Sutradhar, A. (2015). Estimation of vehicle yaw rate and lateral motion for dynamic stability control using Unscented Kalman Filtering (UKF) approach. In *Michael Faraday IET International Summit 2015*, 24–29. DOI:10.1049/cp.2015.1601.

Vahidi, A., Stefanopoulou, A., and Peng, H. (2005). Recursive least squares with forgetting for online estimation of vehicle mass and road grade: theory and experiments. *Vehicle System Dynamics*, 43(1), 31–55. DOI:10.1080/00423110412331290446.